Carnegie Observatories Astrophysics Series, Vol. 3:
Clusters of Galaxies: Probes of Cosmological Structure and Galaxy Evolution, 2004
ed. J. S. Mulchaey, A. Dressler, and A. Oemler (Pasadena; Carnegie Observatories:
http://www.ociw.edu/ociw/symposia/series/symposium3/proceedings.html)

Measuring Evolution and Cosmology from ACS Observations of Clusters

M. POSTMAN[1] et al.
(1) Space Telescope Science Institute, Baltimore, MD, USA

Abstract

Preliminary results from the ACS Guaranteed Time Observers Survey of Galaxy Clusters are presented. The survey includes observations of low-z strongly lensing clusters, intermediate redshift ($0.8 < z < 1.3$) x-ray and optically selected clusters, and high redshift ($z > 2$) radio galaxies believed to reside within forming proto-clusters. Our findings include that there is little evolution in the color-magnitude relation out to $z = 1.24$; that there is now consistency between the mass estimates of A1689 as measured from lensing, kinematics, and x-rays; that interesting constraints on Λ can be achieved by identification of distant multiply lensed galaxies; and new and convincing evidence for a proto-cluster at $z > 4$.

1.1 Introduction

The installation of the Advanced Camera for Surveys (hereafter ACS; Ford et al. 2002) on the Hubble Space Telescope in March 2001 enabled a remarkable new era for space-based imaging of distant galaxies. The enhanced resolution, red sensitivity, and field of view of the wide-field camera on ACS make HST observations of distant galaxy clusters much more efficient and, in particular, enable large mosaics to be constructed to HDF-like depths in only a handful of orbits. These performance improvements to HST's imaging will provide significantly higher quality data than has ever existed in the study of the distribution of cluster dark matter and the evolution of cluster galaxies, particularly for systems at or beyond $z \sim 1$. The ACS Investigation Definition Team (IDT) is using this new opportunity to conduct a comprehensive cluster survey that will focus on addressing three main research areas: precise determination of the dark matter distribution within the central regions of nearby strongly lensing clusters, better constraints on the formation and evolution of early type cluster members from observations of systems at $z \gtrsim 0.8$, and the detection and characterization of high redshift ($z > 2$) proto-clusters. In this talk I will present some preliminary results on each of these topics.

1.2 The ACS IDT Cluster Survey Program

The IDT cluster survey is divided up into 3 redshift ranges. The goals of precise measurement of the distribution of cluster dark matter, observational constraints on Λ, and detection of strongly lensed $z > 4$ galaxies will be accomplished by observing 4 of the strongest lensing, low-z clusters (A1689, A2218, CL0024+1652, and MS1358). Each cluster will be observed in 4 bands over a single ACS/WFC field, reaching a depth of 27.00 in the F675W band, within a few tenths of a magnitude of the depth of the HDF but achieved in $\sim$15% of the exposure time. In addition to the deep observations above, much shorter exposures have been taken for 10 low-z lensing clusters in the SDSS-i and SDSS-z bands in an effort to identify bright lensed i-band dropout galaxies.

The goals of constraining the formation epochs, star formation histories, and scaling relations of early type cluster members as well as the evolution of the different morphological populations in clusters will be accomplished by observing 8 clusters with $0.8 < z < 1.3$ - these clusters include MS1054-03 ($z = 0.83$), RXJ0152-1357 ($z = 0.83$), CL1604+4304 ($z = 0.90$), CL1604+4321 ($z = 0.92$), RXJ0910+5422 ($z = 1.10$), RXJ1252-2927 ($z = 1.24$), RXJ0849+4452 ($z = 1.26$) plus one to be determined shortly. Each of these systems will be observed in at least 2 passbands, roughly straddling the rest-frame 4000Å break (to minimize the k-corrections required to transform the photometry to rest-frame $U-B$ colors). In most cases, at least 3 (and often 4) overlapping pointings are acquired to span the central $1.5h_{70}^{-1}$ Mpc region. The overlap is designed so that the central 1 arc minute of each cluster receives the cumulative exposure time of all the pointings.

Finally, the goals of detecting and characterizing proto-clusters will be achieved by observing 3 or 4 high-z radio galaxies. The objects selected are all associated with overdensities of Lyα emitters, which are consistent with the overdensities expected for proto-clusters (e.g., Miley 2000). The clumpy morphologies of high-z radio galaxies are similar to hierarchical model simulations of forming BCGs (Kauffmann et al. 1993) and their Lyα halos are comparable in size to the outer envelopes of present day cD galaxies (van Ojik 1995). The systems slated for observation include TN J1338-1942 ($z = 4.1$) and TN J0924-2201 ($z = 5.2$). Each system will be observed in at least 3 passbands, with one passband selected to include the redshifted Lyα line. At least one additional system (and possibly two) in the range $2 < z < 3.2$ will be included in the survey. All of the above targets have extensive ground-based observations (including many spectroscopic measurements) as well as a broad range of multi-wavelength imaging to ensure that we achieve our overall objective of providing a comprehensive look at cluster evolution.

1.3 Preliminary Results

We present preliminary results from each of the above sub-programs here. Readers are encouraged to read the more detailed accounts in the literature – specifically, Blakeslee et al. 2003 for our work on the color-magnitude relation in RXJ1252-2927 and Miley, Overzier, et al. 2003 for our work on proto-clusters. The results of our lensing mass model for Abell 1689 (Broadhurst, Benitez, et al. 2004) is in preparation.

1.3.1 The Color-Magnitude Relation in Distant Clusters

Present-day cluster ellipticals are a remarkably well-behaved class of objects, with structural and chemical properties obeying simple power-law scaling relations. But this could not always have been the case in a hierarchical universe. While most galaxy formation models can be tuned to reproduce these relations at $z=0$, a more stringent test lies in reproducing their evolution with redshift. To this end, it is important to study rich clusters out to the highest redshifts, when fractional age differences among the galaxies were proportionately greater. In recent years, deep wide-field optical surveys and deep serendipitous X-ray surveys have uncovered significant numbers of rich galaxy clusters to redshift unity and beyond (see reviews by Postman 2002; Rosati 2004). The many of the distant clusters observed in our program were discovered as part of the ROSAT Deep Cluster Survey

Fig. 1.1. ACS WFC color composite images of the core regions of RXJ0152-1357 ($z = 0.83$; left image) and RXJ1252-2927 ($z = 1.24$; right image). The displayed field sizes are roughly 1 arc minute across, or less than 4% of the full mosaic area. Many of the blue objects in the core of RXJ0152 are strongly lensed galaxies.

(Rosati et al. 1998). Here we present new and significant constraints on the evolution of the “red sequence," based on our $i_{775}$and z_{850}observations of one of the more distant systems, RXJ1252.9–2927 (hereafter RDCS 1252), which is one of the most distant galaxy clusters with solid spectroscopic confirmation. Figure 1.1 shows the central regions of the mosaics obtained for RDCS 1252as well as RDCS 0152 at $z = 0.831$. For these analyses, we adopt the best-fit WMAP cosmology: $(h, \Omega_m, \Omega_L) = (0.71, 0.27, 0.73)$ (Bennett et al. 2003), giving scales of 7.6 kpc per arcsec and 8.4 kpc per arcsec, respectively, at $z = 0.831$ and $z = 1.237$.

The reader is referred to Blakeslee et al. 2003 for details of our photometric measurement methodology and more complete details of our data analyses. Each galaxy in our RDCS 1252galaxy sample was examined and morphologically classified, following a procedure similar to that of Fabricant et al. (2000). Here, we simply distinguish between E, S0, and later types, where the intermediate S0 class indicates the apparent presence of a disk without spiral or other structure. Full details on the classifications for a much larger sample, including the spatial distribution of the various types, will be presented by Postman et al. (2004, in preparation). All galaxies in our initial sample classified as early-type, and not known to be interlopers from their spectra, are included in our CM analysis. Of the 31 known members, 22 are classified as early-type, and we include all of these in our analysis even though one (an S0) happened to lie beyond our 1 Mpc radius cutoff.

We fitted the early-type galaxy CM relations using simple linear least squares; other methods gave very similar results. We estimate the scatter from both the standard RMS and the bi-weight scale estimator (Beers et al. 1990). Figure 1.2 presents the CM relation for the RDCS 1252 galaxies. The fit to the full sample of early-type galaxies with $z_{850} < 24.5$ gives

$$(i\text{–}z) = (0.958 \pm 0.006) - (0.025 \pm 0.006)(z_{850} - 23)\,. \tag{1.1}$$

Results for other subsamples are given in Blakeslee et al. 2003. The mean locations of the CM relations for the elliptical and S0 subsamples agree to well within the errors, while the

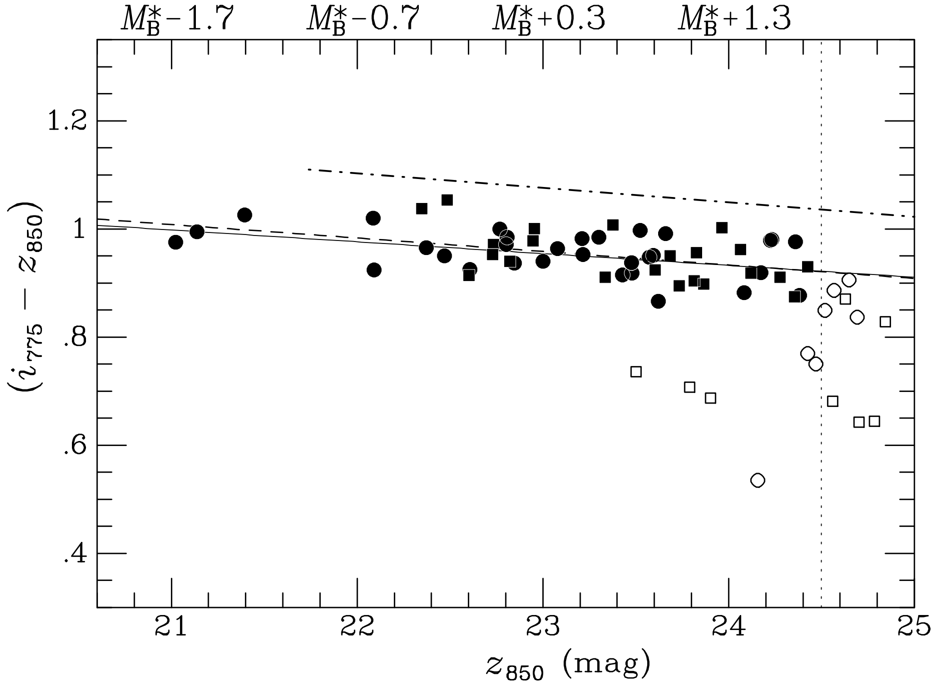

Fig. 1.2. Color-magnitude diagram for early-type galaxies inside $1.9'$ with $(i_{775}–z_{850}) > 0.5$, excluding spectroscopically known interlopers. Circles and squares represent ellipticals and S0s, respectively; solid symbols are used in the CM relation fits, while open symbols (all of which lack spectroscopic information) are rejected as outliers or as below the faint cutoff (indicated by the dotted line). Two representative fits are shown: the fit to the 15 elliptical members (solid line) and to the 52 early-type red-sequence galaxies. The approximate luminosity conversion for RDCS 1252 is shown at top, assuming the WMAP cosmology and −1.4 mag of luminosity evolution as described in the text, such that $M^*_B = -21.7$ (AB). The relation for the Coma cluster, transformed to these bandpasses at $z = 1.24$ (no evolution correction), is indicated by the dot-dashed line.

slopes are consistent at the 1.5-σ level. Eight known late-type members from Rosati et al. (2004, in preparation) for which we have photometry are bluer than the early-type galaxies by 0.25 mag, with a scatter of 0.14 mag about this offset, indicating young stellar populations. We find an intrinsic scatter $\sigma_{\rm int} = 0.023 \pm 0.007$ mag for the 15 confirmed elliptical members. For a limit of $z_{850} < 24.5$, we derive $\sigma_{\rm int} = 0.026$ mag for the clipped sample of 31 ellipticals and $\sigma_{\rm int} = 0.029$ for the 52 E+S0 galaxies. At this limit, the observational errors become dominant and classification is difficult, which could bias our $\sigma_{\rm int}$ estimates. For $z_{850} < 24.0$, still 3 mag down the luminosity function to about $0.3\,L^*$, we find $\sigma_{\rm int} = 0.024$ for 25 ellipticals (with no outliers).

The evolution in $(i_{775}–z_{850})$ at this redshift is complicated at young ages because z_{850} straddles the 4000 Å break and has its blue end near the Balmer jump at 3700 Å. The Balmer jump reaches a maximum at 0.5–1 Gyr, when the relative contribution from A stars is greatest, resulting in a red color at these ages. It is interesting that several of the S0s lie *above* the CM relation, possibly indicating ages < 1 Gyr. As the A star contribution lessens, the color quickly evolves towards the blue, reaching a local minimum near ~ 1.5 Gyr, before commencing a roughly monotonic reddening with age.

We have simulated the $(i_{775}-z_{850})$ colors of galaxies formed under two simple star formation models, similar to those used by van Dokkum et al. (1998). In Model 1, the galaxies form in single bursts randomly distributed over the interval $(t_0, t_{\rm end})$, where t_0 is set to the recombination epoch and $t_{\rm end} < t_z \equiv 5.1$ Gyr, the age of the universe at $z = 1.24$. In Model 2, galaxies form stars at constant rates between randomly selected times (t_1, t_2), where $t_0 < t_1 < t_2 < t_{\rm end}$. We vary $t_{\rm end}$ and at each step calculate colors and luminosities for 10,000 "galaxies" by interpolation and integration of the BC03 solar metallicity models. Assuming $\sigma_{\rm int} = 0.024$ mag for the ellipticals, Model 1 implies a minimum age $t_z - t_{\rm end} = 1.6$ Gyr, i.e., all galaxies finish forming at redshifts $z > z_{\rm end} = 1.9$; the mean luminosity-weighted age is $\tau_L = 3.3$ Gyr (corresponding to $z_L = 3.6$) with a scatter of 30%. Model 2 gives $t_z - t_{\rm end} = 0.53$ Gyr, $z_{\rm end} = 1.4$, and $\tau_L = 2.6$ Gyr (corresponding to $z_L = 2.7$) with 38% scatter. Thus, although some galaxies in Model 2 have formed stars recently, the mean ages are still high. Both models give a mean color $\langle i_{775}-z_{850} \rangle = 0.94$, similar to that observed.

For the S0s, we find $z_{\rm end} = 1.5$ for Model 1 and $z_{\rm end} = 1.3$, indicating recent star formation, and age scatters of 44–47%. Finally, we note that the 1996 version of the BC models would have predicted higher formation epochs, e.g., $z_{\rm end} > 2.5$ and $z_{\rm end} > 2.0$ for the ellipticals in Models 1 and 2, respectively, and an age scatter of only 20%, although the predicted color is then redder by 0.1 mag. Overall, we conclude that the ellipticals are an evolved population, with a mean age $\tau_L \gtrsim 2.6$, a minimum age $\sim 1 \pm 0.5$ Gyr, and an age scatter of (34 ± 15)%, where the error reflects uncertainty in $\sigma_{\rm int}$ and scatter in the models.

To enable comparison with previous work, we convert observed $(i_{775}-z_{850})$ quantities to rest-frame $(U-B)_z$ at $z = 1.24$. Figure 1.3 uses this conversion, and other transformations from van Dokkum et al. (2000), to compare our results to some previous studies of the CM relation in intermediate-redshift clusters. Linear fits to the data shown in Figure 1.3 yield slopes of -0.014 ± 0.010 and 0.003 ± 0.008 for the evolution in the absolute slope and the scatter, respectively. Thus, the scatter is constant, and there is at best marginal evidence for slope evolution, which indicates that the slope is due to a variation in metallicity, not age. Previous studies of cluster samples out to $z \sim 1$ have come to similar conclusions (e.g., Stanford et al. 1998; Kodama et al. 1998; van Dokkum et al. 2000). Van Dokkum et al. (2001) concluded that the slope at $z = 1.27$ was shallower than in the Coma cluster. However, as shown in the figure, our slope measurement is consistent within the errors with both Coma and RX J0848+4453.

The lack of evolution in the CM relation scatter can be explained by progenitor bias (e.g., van Dokkum & Franx 2001): galaxies selected as early-type at any epoch will have old stellar populations, while the later-type progenitors of the youngest ellipticals today will not be selected. The result is an underestimate in the color scatter for the progenitors of modern ellipticals, and thus overestimated ages. An upper limit on the scatter for elliptical progenitors may be estimated from a fit to all confirmed RDCS 1252 members; the result is 3–4 times larger than for the early-type galaxies. We also note that the two central ellipticals themselves, based on their proximity and irregular isophotes, appear likely to undergo dissipationless merger to form a single $\sim 9\,L_B^*$ galaxy, similar to local cD galaxies. We conclude that massive, evolved early-type galaxies were already present in rich clusters at $z = 1.24$. Our simple models imply mean luminosity-weighted ages of 2.6–3.3 Gyr, corresponding to formation at $z = 2.7$–3.6. However, the $(i_{775}-z_{850})$ color is not ideal for the redshift of

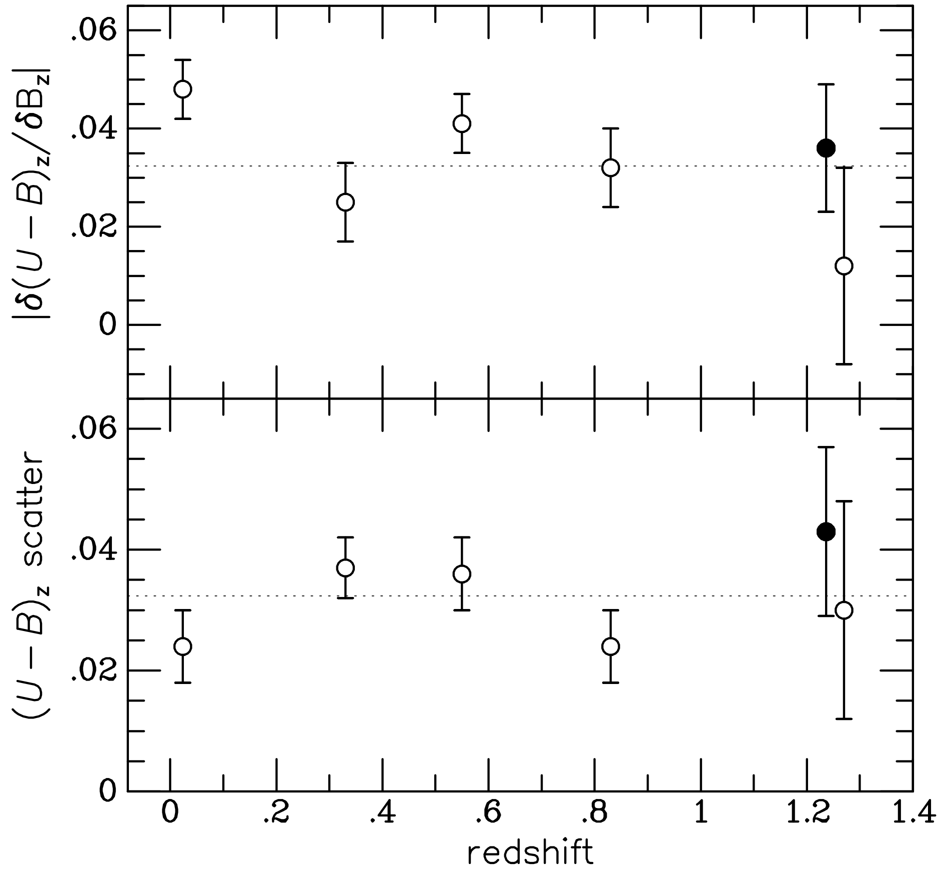

Fig. 1.3. Slope (top) and scatter (bottom) of the rest-frame ($(U{-}B)_z$) CM relation as a function of redshift. The filled circle is from the present work; open symbols show results from, in order of increasing redshift, Bower et al. (1991); van Dokkum et al. (1998); Ellis et al. (1998); van Dokkum et al. (2000); and van Dokkum et al. (2001). The dotted lines indicate the average values.

RDCS 1252, being better suited to measuring the 4000Å break at $z \approx 1.1$. Combining our ACS data with deep, high-resolution near-IR imaging of this field (Lidman et al. 2004) will enable a more robust assessment of early-type galaxy ages. In addition, further studies of the CM relations and morphologies of galaxies in other $z \gtrsim 1$ clusters are needed to improve the constraints on the formation epoch of cluster galaxies and on the evolution of their stellar populations and structural properties.

1.3.2 Gravitational Lensing Mass Model of Abell 1689

Abell 1689 ($z = 0.18$) has the one of the largest Einstein radii known, 40 – 45 arcsec depending on the source redshift, and thus has been the target of much work on measuring the dark matter distribution (Tyson & Fisher 1995; Taylor et al. 1998; Dye et al. 2001; Clowe & Schneider 2001; Xue & Wu 2002). The larger field of view of the WFC on ACS coupled with its higher angular resolution than WFPC2 makes this cluster an obvious choice

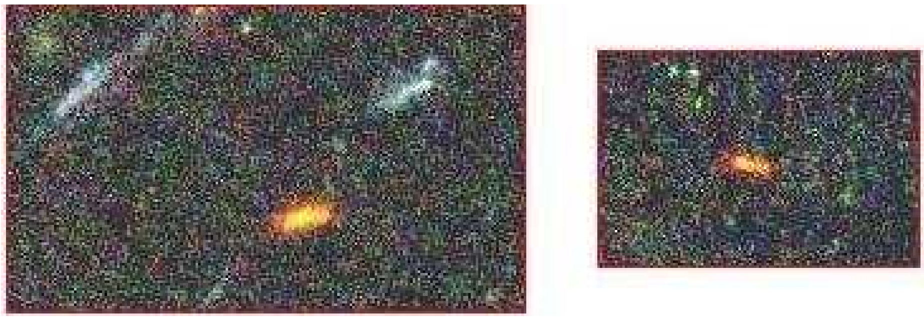

Fig. 1.4. The two images of a multiply lensed $z = 4.86$ galaxy. The redshift has been determined spectroscopically with the Keck Observatory.

for providing a much more reliable gravitational lens mass model than has previously been possible. Prior to our observations, there was a factor of ~ 2 discrepancy between the lensing and x-ray mass (Xue & Wu 2002), with the lensing mass being the larger of the two. We observed A1689 with ACS for a total of 20 orbits in the SDSS-g, r, i, z passbands, reaching a limiting magnitude of 27.4 in g and 27.0 in r.

We obtain an initial mass estimate for A1689 by identifying multiply lensed background galaxies. By identifying such systems with reliably known redshifts, a mass estimate can be derived from the expression $M(\theta < \theta_E) = \theta_E^2 D_d/(8\pi G)$ where θ_E is the angular size of the Einstein radius, D_d is the distance from the observer to the lens, and isothermality is assumed. We identified such a multiply lensed galaxy at a redshift of $z = 4.86$. Figure 1.4 shows the two images of this object. We derive an mass of $(1.56 \pm 0.05) \times 10^{14}\mathrm{M}_\odot$ within the Einstein radius (which corresponds to a radius of 133 kpc in the WMAP cosmology). Translated to a velocity dispersion, this corresponds to 1294 ± 20 km s^{-1}. Compare this with the observed kinematic velocity dispersion of 1439^{+145}_{-96} km s^{-1}(Teague, Carter, & Gray 1990). Our lensing mass estimate now agrees with the kinematic mass and the x-ray mass to within 10%. A more careful modeling of the two dimensional mass distribution, which makes far fewer assumptions about isothermality, is underway by Broadhurst, Benitez, et al. 2004.

One novel aspect of such high quality observations of strongly lensing systems is the ability to identify many multiply lensed objects at many different redshifts. Because the Einstein radius is a function of the ratio of the distance between the lens and source to the distance between the observer and the lens, the Einstein radius will depend on the redshift of the source. Tracing the Einstein radius as a function of redshift for a given system, thus, potentially enables a constraint to be placed on Λ that is completely independent from the SNIa constraints. Figure 1.5 shows a plot of our initial attempt to do just this based on 3 multiply lensed systems at $z = 1.8, 4.3$, and 4.9. We derive the crude constraint of $\Lambda = 0.8^{+0.15}_{-0.30}$. This value is computed assuming the mass distribution follows that for an isothermal sphere. However, a much more interesting constraint will soon be possible by using more arclets – we have recently identified up to 17 multiply lensed systems (with either spectroscopic or photometric redshifts) – and as we relax the isothermal sphere assumption.

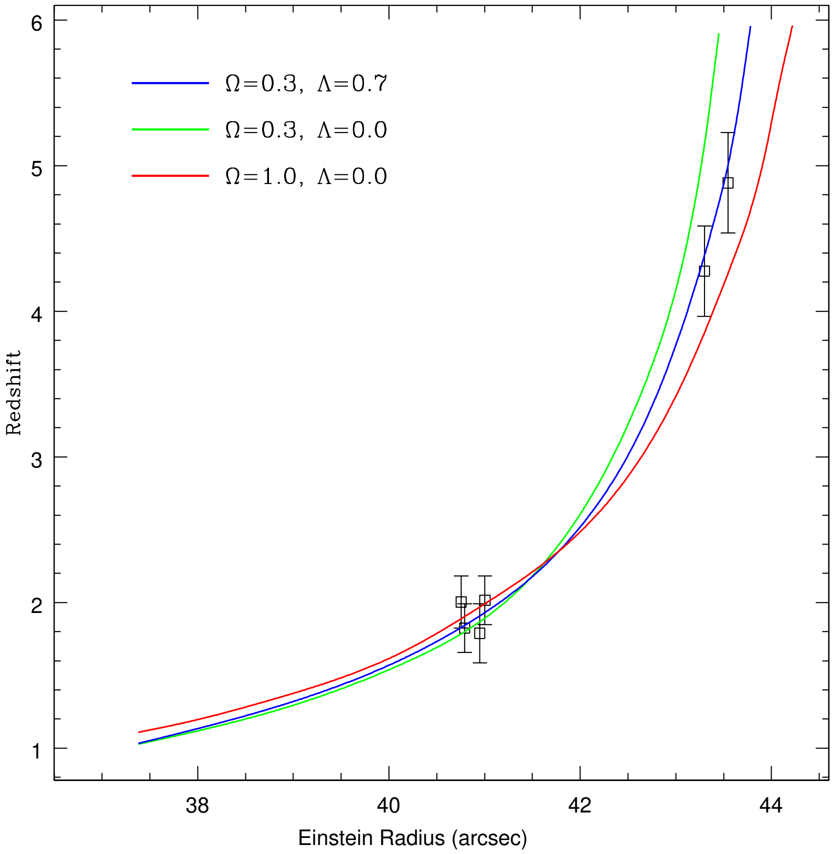

Fig. 1.5. The Einstein radius as a function of redshift for different cosmological models and for 3 different multiply lensed sources.

1.3.3 Evidence for a Proto-cluster at $z = 4.1$

Luminous high redshift radio galaxies (HzRGs) provide an efficient way to detect distant proto-clusters (Miley 2000) and we have dedicated a significant number of orbits to studying these systems. Here I will present our observations of one of the most distant HzRGs, TN J1338-1942, at a redshift of $z = 4.1$. This system has 21 spectroscopically confirmed Lyα emitters. We observed TN1338 for a total of 13 orbits in the SDSS-g,r,i passbands. The goals are to determine the properties of the spectroscopically confirmed Lyα emitters, search for additional Lyman break galaxies (LBGs) associated with the protocluster, and finally to characterize the properties of the HzRG itself. See Miley, Overzier et al. 2003 for details. Figure 1.6 shows a color composite image of the ACS/WFC image of TN1338. All of the known Lyα emitters are detected in r and i but are essentially absent in the g-band, consistent with the presence of Lyman breaks at the protocluster redshift. In addition, there is a significant excess of previously unknown g-band dropouts in the field (by

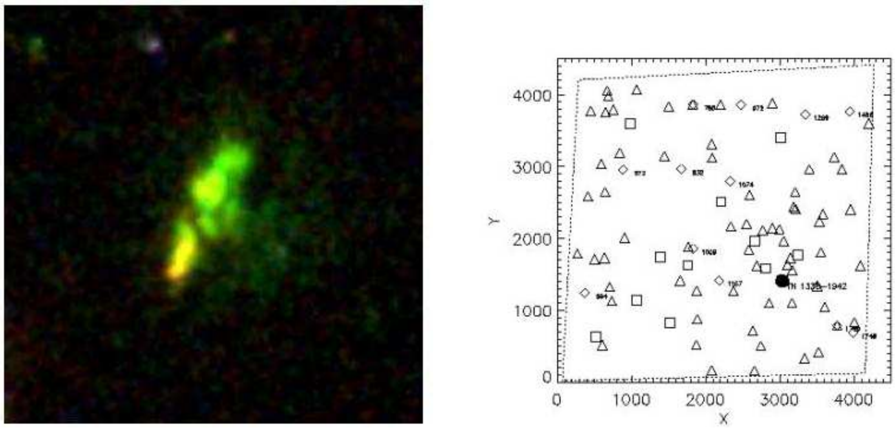

Fig. 1.6. Left: A color composite of the $z = 4.1$ radio galaxy TN1338-1942. The g, r, and i-bands correspond to the blue, green, and red colors. The r-band (green color in the image) contains the redshifted Lyα line. The field of view shown is about 6 arcseconds. Right: the spatial distribution of the newly detected LBGs – they tend to be concentrated around the HzRG (solid black dot).

roughly a factor of 3 – 5 relative to GOODS CDFS) that are concentrated in the 1 arcminute region centered on the HzRG.

The possible relation of the HzRG to the protocluster is important because it is presumed to be the dominant cluster galaxy undergoing assembly. The ACS reveals a significant Lyα halo around this galaxy that extends out to 110 kpc and has an asymmetric morphology that is aligned with the radio source axis and points away from the protocluster center. This orientation indicates that shocks from the outward moving radio het may play a role in ionizing the ambient gas.

1.4 Summary

The Wide Field Camera on the ACS is performing as expected and is proving to be a tremendous tool in the study of galaxy evolution and observational cosmology. The IDT galaxy cluster survey is now yielding new and exciting results in both these fields, only some of which have I had the time to present here. We are finding compelling evidence for protoclusters at $4 < z < 5.5$ and for early and synchronized formation for the early type galaxies that ultimately populate these dense regions. We have also placed more accurate constraints on the central mass of A1689 and are exploring the possibility of providing a new and independent determination of the Λ parameter. I must note that the work presented here is the combined effort of many people on the ACS team. I acknowledge in particular the efforts of John Blakeslee, Marijn Franx, Piero Rosati, Txitxo Benitez, Tom Broadhurst, Roderik Overzier, George Miley, Holland Ford, and Garth Illingworth – all of whom played key roles in developing the above scientific results. The ACS was developed under NASA contract NAS 5-32864, and this research has been supported, in part, by NASA grant NAG5-7697. The STScI is operated by AURA Inc., under NASA contract NAS5-26555.

References

Beers, T. C., Flynn, K., & Gebhardt, K. 1990, AJ, 100, 32
Bennett, C. L. et al. 2003, ApJS, 148, 1
Broadhurst, T., Benitez, N., et al. 2004, in preparation
Bower, R. G., Lucey, J. R., & Ellis, R. S. 1992, MNRAS, 254, 589
Clowe, D., & Schneider, P. 2001, A&A, 379, 384
Dye, S., Taylor, A. N., Thommes, E. M., Meisenheimer, K., Wolf, C., & Peacock, J. A. 2001, MNRAS, 321, 685
Ellis, R. S., Smail, I., Dressler, A., Couch, W. J., Oemler, A. J., Butcher, H., & Sharples, R. M. 1997, ApJ, 483, 582
Fabricant, D., Franx, M., & van Dokkum, P. 2000, ApJ, 539, 577
Ford, H. C. et al. 2002, Proc. SPIE, 4854, 81
Kauffmann, G., White, S. D. M., Guiderdoni, B. 1993, MNRAS, 264, 201
Lidman, C. et al. 2004, A&A, submitted
Miley, G. 2000, in From Extrasolar Planets to Cosmology: the VLT Openning Symposium, eds. J. Bergeron and A. Renzini, 32
Miley, G., Overzier, R., et al. 2003, Nature, in press.
Postman, M. 2002, ASP Conf. Ser. 268, 3
Postman, M. et al. 2004, in preparation
Rosati, P., della Ceca, R., Norman, C., & Giacconi, R. 1998, ApJ, 492, L21
Rosati, P. 2004, in Clusters of Galaxies: Probes of Cosmological Structure and Galaxy Evolution (Cambridge: Cambridge Univ. Press), in press
Rosati, P. et al. 2004, AJ, submitted
Stanford, S. A., Eisenhardt, P. R., & Dickinson, M. 1998, ApJ, 492, 461
Taylor, A. N., Dye, S., Broadhurst, T. J., Benitez, N., & van Kampen, E. 1998, ApJ, 501, 539
Teague, P., Carter, D., Gray, P. M. 1990, ApJS, 72, 71
Tyson, J. A., & Ficsher, P. 1995, ApJ, 446, L55
van Dokkum, P. G., Franx, M., Kelson, D. D., Illingworth, G. D., Fisher, D., & Fabricant, D. 1998, ApJ, 500, 714
van Dokkum, P. G., Franx, M., Fabricant, D., Illingworth, G. D., & Kelson, D. D. 2000, ApJ, 541, 95
van Dokkum, P. G., Stanford, S. A., Holden, B. P., Eisenhardt, P. R., Dickinson, M., & Elston, R. 2001, ApJ, 552, L101
van Dokkum, P. G. & Franx, M. 2001, ApJ, 553, 90
van Dokkum, P. G. & Stanford, S. A. 2003, ApJ, 585, 78
van Ojik, R. 1995, Ph.D. Thesis, Leiden University, Leiden
Xue, S. & Wu, X. 2002, ApJ, 576, 152.